

## Resolving single cone inputs to visual receptive fields

Lawrence C Sincich<sup>1</sup>, Yuhua Zhang<sup>2,3</sup>, Pavan Tiruveedhula<sup>2</sup>,  
Jonathan C Horton<sup>1</sup> & Austin Roorda<sup>2</sup>

**With the current techniques available for mapping receptive fields, it is impossible to resolve the contribution of single cone photoreceptors to the response of central visual neurons. Using adaptive optics to correct for ocular aberrations, we delivered micron-scale spots of light to the receptive field centers of neurons in the macaque lateral geniculate nucleus. Parvocellular LGN neurons mapped in this manner responded with high reliability to stimulation of single cones.**

Human vision is subserved by three types of cone photoreceptors that differ in spectral sensitivity, in density with respect to distance from the fovea and in relative abundance across individuals<sup>1</sup>. Because the receptive field centers of most neurons in the early visual system are composed of multiple cones, the question arises of whether the stimulation of just one cone is sufficient to activate retinal ganglion cells and, consequently, for stimuli to be perceived. Moreover, given the dispersal of photoreceptor signals through the retinal layers<sup>2</sup>, it is likely that different cones will vary in their efficacy at driving downstream neural activity. We found that thalamic responses could be reliably mapped by stimulating individual cones and that the probability of evoking a spike with each stimulus flash varied, in part because of exquisite sensitivity to the position of stimuli relative to each cone.

Ordinarily, a neuron's response properties are characterized by presenting stimuli on a screen while recording action potentials with an extracellular electrode<sup>3</sup>. This yields a receptive field that is delimited in time and space, indicating which stimuli are effective at driving the cell. Such a method does not provide direct identification of the cones feeding the receptive field. This method is also limited by optical aberration, diffraction, scatter, pre-retinal absorption and eye movement, all of which degrade visual stimuli. These limitations alter the location and spectral intensity of light impinging on the photoreceptors, making it difficult to map the cone field precisely, especially near the fovea, where cone spacing is only a few microns. To overcome these difficulties, we used an adaptive optics scanning laser ophthalmoscope (AOSLO) to visualize and directly stimulate the cones *in vivo* in the macaque<sup>4,5</sup> (details in **Supplementary Methods**). Experiments were conducted using procedures approved by the University of California San Francisco Institutional Animal Care and Use Committee, in accordance with US National Institutes of Health guidelines. Neurons were recorded in the lateral geniculate nucleus

(LGN), allowing us to explore receptive field properties that cannot be examined with traditional mapping techniques.

As expected from the retinotopic organization of the LGN, an orderly sequence of receptive fields was recorded in the left eye during an electrode penetration (**Fig. 1a**). Superimposed on the fundus photograph is a montage of AOSLO cone images (each image is  $1.2^\circ \times 1.2^\circ$ ) used to aid navigation in the retina when searching for responsive cones. Once an LGN neuron was encountered, the first task was to find the retinal location where a flashed stimulus generated a response. We identified which cones produced the briskest firing by moving a flickering spot across the retina, which was a straightforward procedure because the cones being stimulated could be seen in real time (**Supplementary Video 1**).

The diameter of the cone field was then determined by plotting the neural response profile obtained by flashing a smaller stimulus pseudo-randomly at locations spaced every 3  $\mu\text{m}$  through the middle of the field (**Fig. 1b**). These 3- $\mu\text{m}$  square stimuli subtended 52 arcsec, which is approximately equal to the diameter of one cone's inner segment at  $3.7^\circ$ , the eccentricity of this parvocellular ON-center field. Because the stimuli were constructed from a 30-Hz raster scan, the neural response was phase-locked to the frame rate, with the flash duration at each locus being about 5  $\mu\text{s}$  (see **Supplementary Fig. 1** for details). To control for retinal motion, we used a video-based algorithm to track cone positions (**Supplementary Video 2** and **Supplementary Fig. 2**). Single stimulus flashes delivered to single cones reliably led to LGN spikes, with the likelihood of generating any spikes reaching 85% at the peak response location. Responses diminished sharply at the edge of the cone field, where a shift in the stimulus position of just 3  $\mu\text{m}$  dropped the LGN spike probability to baseline, suggesting that light delivery was not affected seriously by optical blur or intra-retinal scatter. Toward the limits of the tested area, the probability of firing began to dip below the baseline level, presumably reflecting inhibition from the receptive field surround.

The response profile of neuron 1 (**Fig. 1b**) has variation in the spike probability at each stimulus location, particularly in the receptive field center. There are several possible sources for this variation. First, although parvocellular neurons are dominated by a single cone type, it is unclear whether this property arises from only one cone type being wired up to the field center or if one cone type simply outnumbers the others<sup>6–8</sup>. With the narrowband light that we used for stimulation (centered at a 680-nm wavelength), *in vitro* measurements of macaque spectral sensitivities would predict that L cones are 14-fold more sensitive than M-cones and  $10^{5.8}$ -fold more so than S cones<sup>9</sup>. However, the relationship between sensitivity differences and firing rate differences in downstream neurons is unclear, as neural responses often sum nonlinearly. Second, the synaptic weighting of the input from each cone to a ganglion cell, even from cones of the same type, may not be equal. Such variation in synaptic efficacy would be transmitted from

<sup>1</sup>Beckman Vision Center, University of California, San Francisco, San Francisco, California, USA. <sup>2</sup>School of Optometry, University of California, Berkeley, Berkeley, California, USA. <sup>3</sup>Department of Ophthalmology, University of Alabama, Birmingham, Alabama, USA. Correspondence should be addressed to L.C.S. (sincichl@vision.ucsf.edu).

Received 10 March; accepted 20 May; published online 28 June 2009; doi:10.1038/nn.2352

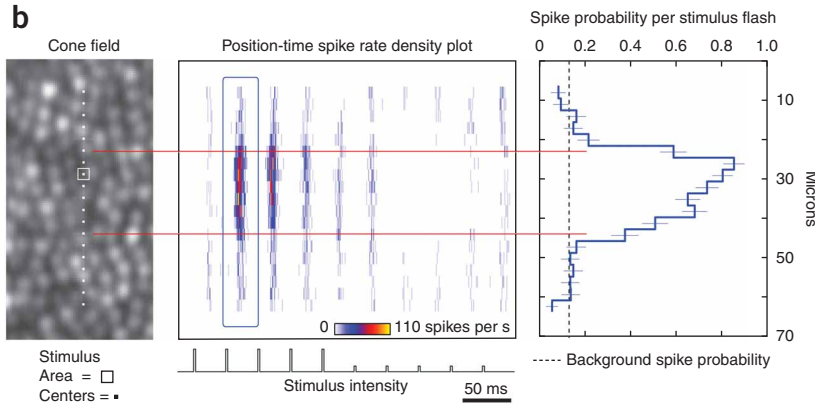
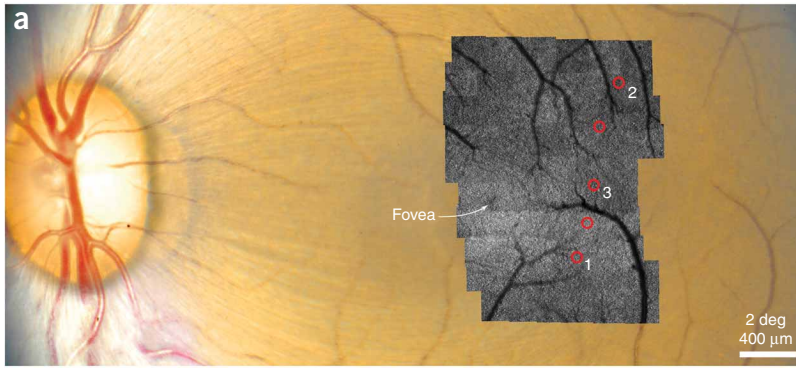


**Figure 1** Localizing cone fields of LGN neurons. (a) Left eye fundus photograph with AOSLO images shown as a montage over the macula where receptive fields (red circles) were recorded. The neurons analyzed are numbered for reference. (b) Stimuli flashed at 19 contiguous locations across the cone field of neuron 1 (left) led to an adapting ON response and an inhibitory OFF response (middle, each row in the spike density plot represents the temporal response of one position in the cone field). Response latency was ~45 ms. The cone field is rotated 90° for display purposes. Residual light in the optical path generated background activity at the frame rate. Activity above the background rate occurred over a region spanning four cones, indicated by red lines. Mean spike probability (right, ± s.e.m.) was measured in the blue outlined area of the spike density plot. Micron scale applies to all panels.

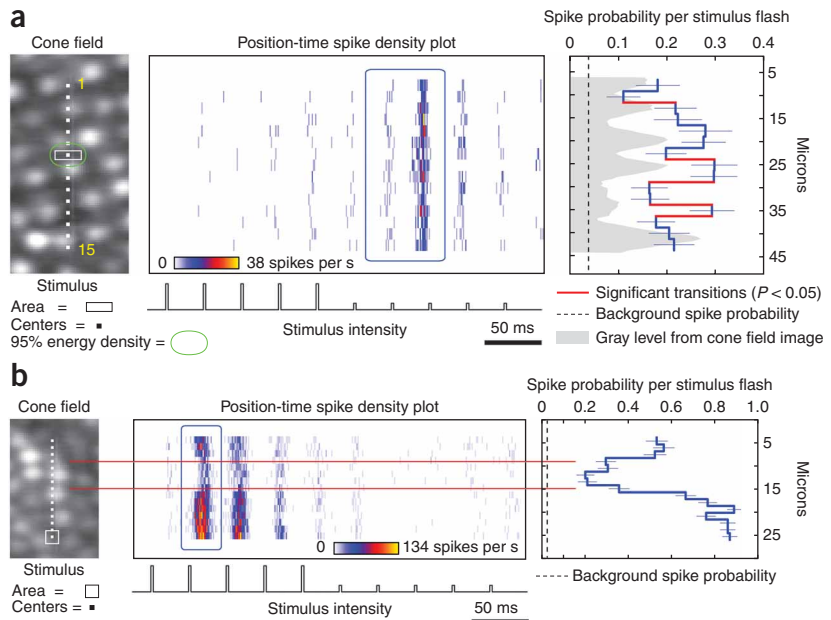
was smaller than the gap between cones in the adaptive optics images (Fig. 2a). In this OFF-center cell, stimuli that impinged on a single cone (positions 8 and 9) generated the largest response, whereas flanking stimuli that landed between cones (for example, positions 7 and 10) evoked significantly fewer spikes ( $P < 0.05$ , one-tailed Fisher's exact test). The response did not go to baseline at the flanks because a fraction of light still landed on the adjacent cone profiles, as shown by the time-averaged energy distribution of the stimulus. As with the other LGN neurons that we recorded, some cones generated significantly different responses, even when stimuli were positioned over them in a similar fashion (for example, responses at positions 8 and 14 in Fig. 2a;  $P < 0.05$ , one-tailed Fisher's exact test), implying that this neuron either received input from both L and M cones or had mixed cone weights. It is worth noting that cone-to-cone electrical coupling is present<sup>11</sup>, which will reduce the apparent discreteness of the stimuli

ganglion cells to LGN neurons. Finally, a substantial source of variation could be the sensitivity of cones to the exact position of the stimulus, an effect that is heightened by their light-guide properties<sup>10</sup>.

To examine the sources of variability in more detail, it was crucial to first measure how well stimuli were restricted to single cones. As a direct test of the spatial effect of a stimulus spot, we recorded responses 6° from the fovea, where cones are more widely spaced. If intra-retinal scatter were minimal and the adaptive optics-corrected spots were small enough, stimuli targeted between cones would be unlikely to drive responses effectively. We flashed rectangular stimuli that had a narrow dimension that

landed on the adjacent cone profiles, as shown by the time-averaged energy distribution of the stimulus. As with the other LGN neurons that we recorded, some cones generated significantly different responses, even when stimuli were positioned over them in a similar fashion (for example, responses at positions 8 and 14 in Fig. 2a;  $P < 0.05$ , one-tailed Fisher's exact test), implying that this neuron either received input from both L and M cones or had mixed cone weights. It is worth noting that cone-to-cone electrical coupling is present<sup>11</sup>, which will reduce the apparent discreteness of the stimuli

**Figure 2** Parvocellular LGN activity varies with stimulus position and cone type. (a) Narrow 1.5- × 6-μm stimuli flashed at 15 positions resulted in OFF responses in neuron 2 that were highest when stimuli landed on a cone (for example, position 8) and were significantly reduced when stimuli fell between cones (red transitions,  $P < 0.05$ , one-tailed Fisher's exact test). The green contour shows the region where 95% of the time-averaged light energy was delivered for this stimulus, taking into account the point-spread function and motion remaining after stabilization. The targeted stimulus area (white) contained 66% of the delivered light. (b) Stimuli flashed at 15 overlapping positions yielded differential responses in neuron 3 that depended on the cone being stimulated. The lowest response corresponded to one cone, indicated between the red lines. For all panels, mean probability per stimulus flash (± s.e.m.) was computed for the blue outlined areas in the spike density plots. Micron scale applies to each row of panels.



actually delivered to the retina because coupled cones can funnel activity through single midget bipolar cells.

Variable response levels for different cones were found in all parvocellular LGN neurons ( $n = 6$ ) and appeared more discrete when stimuli were kept small and positioned in small increments. The cone field for neuron 3, a parvocellular ON-center cell (Fig. 2b), was probed with a 3- $\mu\text{m}$  stimulus at twice the spatial resolution used for neuron 1 (Fig. 1b). As the stimulus was shifted from cone to cone, the spike activity stepped to several distinct levels. The lowest response, which also showed a temporal delay, coincided with the extent of one cone, but was still above the background firing rate. This difference in spatiotemporal firing pattern suggests that an M cone was at this location, whereas the flanking higher responses probably originated from L cones. However, as mentioned earlier, it is also possible that color-tuned neurons are supplied by cones of the same type that differ in input strength. An instrument that allows stimulation with multiple wavelengths to facilitate direct assessment of the spectral tuning in each cone could address this issue.

Because LGN neurons respond reliably when only one of their cone inputs is stimulated, it suggests that single cone activation is sufficient for perception, even away from the fovea. This is supported by data showing that frequency-of-seeing curves asymptote well below 100% when small adaptive optics-corrected spots are flashed in a human subject missing a subpopulation of cones, as stimuli occasionally land in 'holes' in the photoreceptor mosaic<sup>12</sup>. In normal subjects, frequency-of-seeing curves are also liable to be affected when such stimuli fall between cones<sup>13</sup>. With the ability to probe visual responses *in vivo* at their elemental level, the single cone, it will be possible to investigate how variable cone weighting leads to the deviations from cone 'purity' seen for color-sensitive neurons in the LGN<sup>14</sup> and primary visual cortex<sup>15</sup>.

Note: Supplementary information is available on the Nature Neuroscience website.

#### ACKNOWLEDGMENTS

We thank Q. Yang, D.W. Arathorn and M. Feusner for help with software development, and D. Williams and D. Copenhagen for insightful manuscript comments. This work was supported by National Eye Institute grants EY10217 (J.C.H.), EY014375 (A.R.) and EY02162 (Beckman Vision Center). Support was also received from the National Science Foundation, through grant IIS-0712852 (L.C.S.), the Center for Adaptive Optics cooperative agreement AST-9876783, managed by University of California Santa Cruz, and Research to Prevent Blindness. The California Regional Primate Research Center is supported by US National Institutes of Health Base Grant RR00169.

#### COMPETING INTERESTS STATEMENT

The authors declare competing financial interests: details accompany the full-text HTML version of the paper at <http://www.nature.com/natureneuroscience/>.

Published online at <http://www.nature.com/natureneuroscience/>.

Reprints and permissions information is available online at <http://www.nature.com/reprintsandpermissions/>.

- Hofer, H., Carroll, J., Neitz, J., Neitz, M. & Williams, D.R. *J. Neurosci.* **25**, 9669–9679 (2005).
- Wässle, H. *Nat. Rev. Neurosci.* **5**, 747–757 (2004).
- Hubel, D.H. & Wiesel, T.N. *J. Physiol. (Lond.)* **160**, 106–154 (1962).
- Roorda, A. *et al. Opt. Express* **10**, 405–412 (2002).
- Arathorn, D.W. *et al. Opt. Express* **15**, 13731–13744 (2007).
- Wiesel, T.N. & Hubel, D.H. *J. Neurophysiol.* **29**, 1115–1156 (1966).
- Diller, L. *et al. J. Neurosci.* **24**, 1079–1088 (2004).
- Buzás, P., Blessing, E.M., Szmajda, B.A. & Martin, P.R. *J. Neurosci.* **26**, 11148–11161 (2006).
- Baylor, D.A., Nunn, B.J. & Schnapf, J.L. *J. Physiol. (Lond.)* **390**, 145–160 (1987).
- Roorda, A. & Williams, D.R. *J. Vis.* **2**, 404–412 (2002).
- Hornstein, E.P., Verweij, J. & Schnapf, J.L. *Nat. Neurosci.* **7**, 745–750 (2004).
- Makous, W. *et al. Invest. Ophthalmol. Vis. Sci.* **47**, 4160–4167 (2006).
- Wesner, M.F., Pokorny, J., Shevell, S.K. & Smith, V.C. *Vision Res.* **31**, 1021–1037 (1991).
- Reid, R.C. & Shapley, R.M. *J. Neurosci.* **22**, 6158–6175 (2002).
- Johnson, E.N., Hawken, M.J. & Shapley, R. *J. Neurophysiol.* **91**, 2501–2514 (2004).